J Mol Med (2008) 86:1243–1254
DOI 10.1007/s00109-008-0388-1

ORIGINAL ARTICLE

Multiple therapeutic effects of valproic acid in spinal muscular atrophy model mice

Li-Kai Tsai · Ming-Shiun Tsai · Chen-Hung Ting · Hung Li

Received: 27 April 2008 / Revised: 9 July 2008 / Accepted: 9 July 2008 / Published online: 23 July 2008

Abstract Spinal muscular atrophy (SMA) is a progressive disease involving the degeneration of motor neurons with no currently available treatment. While valproic acid (VPA) is a potential treatment for SMA, its therapeutic mechanisms are still controversial. In this study, we investigated the mechanisms of action of VPA in the treatment of type III-like SMA mice. SMA and wild-type mice were treated with VPA from 6 to 12 months and 10 to 12 months of age, respectively. Untreated SMA littermates and age-matched wild-type mice were used for comparison. VPA-treated SMA mice showed better motor function, larger motor-evoked potentials, less degeneration of spinal motor neurons, less muscle atrophy, and better neuromuscular junction innervation than non-treated SMA mice. VPA elevated SMN protein levels in the spinal cord through *SMN2* promoter activation and probable restoration of correct splicing of *SMN2* pre-messenger RNA. VPA also increased levels of anti-apoptotic factors, Bcl-2 and Bcl-x_L, in spinal neurons. VPA probably induced neurogenesis and promoted astrocyte proliferation in the spinal cord of type III-like SMA mice, which might contribute to therapeutic effects by enhancing neuroprotection. Through these effects of elevation of SMN protein level, anti-apoptosis, and probable neuroprotection, VPA-treated SMA mice had less degeneration of spinal motor neurons and better motor function than untreated type III-like SMA mice.

Keywords Animal model · Apoptosis · Motor neuron disease · Neurogenesis · Spinal muscular atrophy · Valproic acid

Abbreviations

ALS	amyotrophic lateral sclerosis
ATPase	adenosine triphosphatase
BrdU	bromodeoxyuridine
ChAT	choline acetyltransferase
CMAP	compound muscle action potential
GFAP	glial fibrillary acidic protein
HDAC	histone deacetylase
NeuN	neuronal nuclear
SMA	spinal muscular atrophy
SMN	survival motor neuron
VPA	valproic acid
vWF	von Willebrand factor

Introduction

Spinal muscular atrophy (SMA) is characterized by the degeneration of spinal motor neurons and is associated with

Electronic supplementary material The online version of this article (doi:10.1007/s00109-008-0388-1) contains supplementary material, which is available to authorized users.

L.-K. Tsai
Department of Neurology,
National Taiwan University Hospital and National Taiwan University College of Medicine,
Taipei 100, Taiwan

M.-S. Tsai
Department of Bioindustry Technology, Da-Yeh University,
Dacun,
Changhua 515, Taiwan

C.-H. Ting · H. Li (✉)
Institute of Molecular Biology, Academia Sinica,
Nankang,
Taipei 115, Taiwan
e-mail: hungli@ccvax.sinica.edu.tw

H. Li
Department of Neurology, Center for Neuropsychiatry,
China Medical University and Hospital,
Taichung 404, Taiwan

muscle paralysis and atrophy. Currently, no curative treatment is available for SMA. Childhood SMA exhibits an autosomal recessive pattern of inheritance and most SMA patients have gene deletions, mutations, or conversions of the telomeric copy of the *survival of motor neuron* gene (*SMN1* [MIM 600354]). The centromeric *SMN* gene (*SMN2* [MIM 601627]) is still present in all of these SMA patients but is not able to compensate for the *SMN1* gene defect as most of the *SMN2* gene product is defectively spliced [1, 2].

Valproic acid (VPA), a histone deacetylase (HDAC) inhibitor, increased SMN protein levels in cells derived from SMA patients [3, 4]. SMA mice also showed less degeneration of spinal motor neurons after VPA treatment [5]. Furthermore, VPA increased *SMN* messenger RNA in 70% of SMA gene carriers and 35% of SMA patients in vivo [6]. VPA also improved muscle strength in some SMA patients [7, 8]. Currently, a phase II clinical trial of VPA in SMA is ongoing [9], and SMA-related physicians and patients are becoming more interested in VPA. However, the therapeutic mechanisms of VPA in treating SMA are still not fully understood.

VPA promoted neurite outgrowth independently from regulation of the SMN protein [10]. VPA treatment increased the level of Bcl-2 in the frontal cortex of rats [11, 12]. In addition, VPA induced neurogenesis in the dentate gyrus of the rat hippocampus [13]. Furthermore, another HDAC inhibitor, trichostatin A, increased survival times in SMA mice and induced muscle regeneration in the injured muscles of mice in another study [14, 15]. Understanding the therapeutic mechanisms of VPA may not only reveal new targets for disease treatment, but may also suggest other treatments for related diseases. In this study, we investigated the therapeutic effects of VPA in our SMA mice.

Materials and methods

Mice

We have previously generated SMA-like mice via a homozygous knock-out of *Smn* exon 7 with transgene of human *SMN2* ($Smn^{-/-}SMN2^{+/-}$) [16]. We further obtained type III-like specific SMA mice by purification of the genetic background (C57BL/6J) from the original mice (*SMN2* copy number of two, heterozygous, confirmed by Southern blots). The life span of these mice is 13±2 months [17], and they first show signs of spinal motor neurons degeneration from 6 months of age [5].

Mice were supplied with sterile water and rodent pellets ad libitum (two to three per cage), and were reared in the Laboratory Animal Center of the National Taiwan University College of Medicine, Taiwan. Mice were randomly assigned to treated and untreated groups. SMA and wild-type mice were treated with VPA from 6 to 12 months and 10 to 12 months of age, respectively. Untreated SMA littermates and age-matched wild-type ($Smn^{+/+}SMN2^{-/-}$, same strain) mice were used for comparison. Though we did not initially include a study of VPA-treated wild-type mice, this arm was added later for further comparisons: the VPA treatment period in the wild-type mice was therefore only from 10 to 12 months. In treated mice, VPA (valproic acid sodium salt; Sigma, St. Louis, MO, USA) was added to the daily drinking water at 0.2 mg/ml. These mice consumed 6–10 ml of water per day, corresponding to a total VPA consumption of approximately 40–75 mg/kg/day. All procedures were approved by the National Taiwan University College of Medicine, Institutional Animal Care and Use Committee, Number #20050056.

Motor function tests

Four sets of functional tests were used to evaluate the motor function of mice as previously described [5]. Briefly, in the tilting test the mice were placed on a progressively tilting wooden platform. The highest degree of inclination at which the mice could hold on for 5 s was recorded. In the wheel running test, the mice were placed in a running wheel and the number of cycles run by the mouse per minute was counted. For the RotaRod maintenance test, the mice were placed on a RotaRod, while the rolling rate of the transverse rod was increased and the time each mouse remained on the rod was recorded. In the landing foot spread test, the mouse was dropped from a height of 30 cm above the bench, and the position of ink marks from the pre-inked fourth digit of each hind limb upon landing was measured.

Electrophysiological study

Detailed methods for electrophysiological study have been reported previously [5]. Briefly, supramaximal pulses were delivered to a pair of bipolar electrodes on the exposed sciatic nerve at the sciatic notch. An active recording bipolar needle electrode was inserted in the gastrocnemius muscle. Compound muscle action potentials (CMAP) were recorded as biphasic waves, and the peak-to-peak amplitude was measured.

Pathology

For immunohistochemistry, the lumbar spinal cord and muscle were removed, fixed in 10% formaldehyde at room temperature for 3 h, placed in 15% sucrose for 3 h, then in 30% sucrose at 4°C overnight, and then flash-frozen in liquid nitrogen-cooled isopentane. Serial sections (spinal cord

7 μm; muscle 15 μm; at least 20 sections per mouse) were cryocut, blocked with 5% serum, and then incubated overnight at 4°C with the following primary antibodies: anti-choline acetyltransferase (ChAT; 1:500; Chemicon, Temecula, CA, USA), anti-neurofilament H 200 kDa (1:200; Chemicon), anti-SMN (1:500; exon 2 epitope, labeling both SMN1 and SMN2 protein; BD, Franklin Lakes, NJ, USA), anti-neuronal nuclear antigen (NeuN; 1:50; Chemicon), anti-Bcl-2 (1:200; Cell Signaling, Beverly, MA, USA), anti-Bcl-x_L (1:200; Cell Signaling), anti-glial fibrillary acidic protein (GFAP; 1:300; Chemicon), and anti-von Willebrand factor (vWF; 1:50; Sigma), or with α-bungarotoxin Alexo Fluor 555 conjugate (1:1,000; Invitrogen, Carlsbad, CA, USA). Samples were then washed with Tris-buffered saline with Tween 20 (TBS-T; 10 mM Tris–HCl, pH 8.0, 150 mM NaCl, and 0.1% Tween 20) and incubated for 1 to 3 h at room temperature with the appropriate fluorescence dye-conjugated secondary antibodies (1:500; Molecular Probes, Eugene, OR, USA), then washed with TBS-T. DAPI (Sigma) was used for nucleus staining. Tissues were examined on a fluorescence microscope (IX70; Olympus Optical Co., Japan) fitted with a SPOT cooled color digital camera and SPOT software v2.2 (Diagnostic Instruments, Sterling Heights, MI, USA) or a LSM510 laser-scanning confocal microscope (Carl Zeiss, Gottingen, Germany).

Detailed methods for H&E staining and neuronal analysis have been reported previously [5]. Briefly, the numbers of neurons showing nuclei were counted in the anterior horn and categorized according to their cell size (400–600, 600–900, and >900 μm^2) and neuronal densities were calculated for each size category.

For retrograde motor neuronal tracing, mice were anesthetized intraperitoneally with 60 mg/kg of pentobarbital and then a total volume of 20 μl of fluorogold (Fluorochrome, Denver, CO, USA) was injected in bilateral gastrocnemius muscles using a 30 G × 1/2 needle and a 100-μl microsyringe (ITO, Fuji, Japan) at a speed of 1 μl/min. Mice were then returned to their cage and 1 week later were processed for histological analysis.

For muscle fiber-type analysis [18], muscle cryosections were pre-incubated in acetate buffer (pH 4.3) at room temperature for 10 min. Then, the myofibrillar adenosine triphosphatase (ATPase) reaction was carried out in ATP incubation medium (1.6 mg/ml ATP, 0.1 M sodium barbital, 0.18 M calcium chloride, pH 9.4) at 37°C for 20 min, 1% calcium chloride at room temperature for 3 min, then 2% cobalt chloride for 3 min, and finally 1% ammonium sulfide for 3 min.

Western blot analysis

Detailed methods for Western blot analysis have been previously reported [19]. Briefly, mouse spinal cords were dissected out and immediately homogenized in RIPA buffer. After centrifugation, the supernatants were collected, separated, and subsequently electrotransferred to polyvinylidene fluoride transfer membrane. The blotting membranes were blocked and then incubated with the primary antibody (anti-SMN/1:1,000; anti-Bcl-2/1:50, Santa Cruz Biotech, Santa Cruz, CA, USA; anti-Bcl-x_L/1:500; anti-Htra2-β1/1:1,000, Abnova, Taipei, Taiwan; anti-phospho-ERK42/44/1:1,000, BD; anti-ERK42/44/1:5,000, Upstate, Lake Placid, NY, USA; anti-phospho-STAT5A/B/1:1,000, Upstate; anti-STAT5A/5B/1:1,000, Upstate; anti-α-tubulin/1:4,000, Santa Cruz Biotech) overnight. The membranes then were washed and incubated with the HRP-conjugated secondary antibody at 1:5,000 dilution (Chemicon). The signals were visualized by autoradiography using enhanced chemiluminescence and then quantified by densitometry using AlphaEase (Alpha Innotech, San Leandro, CA, USA).

Analysis of *SMN2* transgene expression

Methods for real-time polymerase chain reaction (PCR) were as described previously [20]. Total RNA was extracted from homogenized spinal cord and then converted to cDNA. Quantitative PCR reactions were run in triplicate for each primer set on a Roche LightCycler 1.5 (Roche, Basel, Switzerland). Two *SMN* primer sets, *SMN+7* (designed to amplify *SMN* transcript containing exon 7) and *SMNΔ7* (designed to amplify *SMN* transcript lacking exon 7) and an endogenous *Actin* control primer were used on each sample. A mouse "calibrator" sample was run on the plate and the value for this sample was set to 1.

Bromodeoxyuridine labeling

Bromodeoxyuridine (BrdU, Sigma) was used for mitotic labeling. For analysis of neurogenesis, SMA mice were injected intraperitoneally with BrdU (100 mg/kg) at 11 months of age every 12 h for 3 days. After VPA (n=4) or no treatment (n=4) for 4 weeks, the mice were killed and spinal cord was removed for analysis (20–30 sections per mouse). For myogenesis analysis, BrdU (150 mg/kg) was injected intraperitoneally in SMA mice at 12 months with (n=3) or without 6-month VPA treatment 6 h before sacrifice. BrdU immunohistochemistry procedures using specific antibody raised against BrdU (1:200; Chemicon) have been previously described [21].

Statistical analysis

Values are expressed as mean ± SEM. Data from the many individual sections of spinal cord and muscles taken from one mouse were averaged before comparison. A Wilcoxon's rank-sum test was used to determine the significance of

differences in continuous data between groups. Two-tailed P values of less than 0.05 were considered statistically significant. STATA software (version 8.0; Stata, TX, USA) was used for the statistical analyses.

Results

Motor function and morphology

SMA and wild-type mice were treated with VPA from 6 to 12 months and 10 to 12 months of age, respectively. Untreated SMA littermates and age-matched wild-type mice were used for comparison. Motor function was measured with four different tests in SMA and wild-type mice at 6 months of age. Motor performance was similar in all four groups before treatment. At 12 months, VPA-treated mice had significantly better motor function than untreated SMA mice (Fig. 1a; P=0.02), and there was no significant difference between motor performance in the treated SMA and wild-type groups, except in wheel running scores (P=0.01).

The SMA mice used here generally show obvious muscle atrophy by 9 months of age [5]. In a comparison using the ratio of gastrocnemius muscle mass to whole body mass as an index of distal muscle atrophy, there was no difference in body mass between all groups at 12 months of age, but the gastrocnemius muscle was significantly smaller in untreated SMA mice (Fig. 1b; P=0.02).

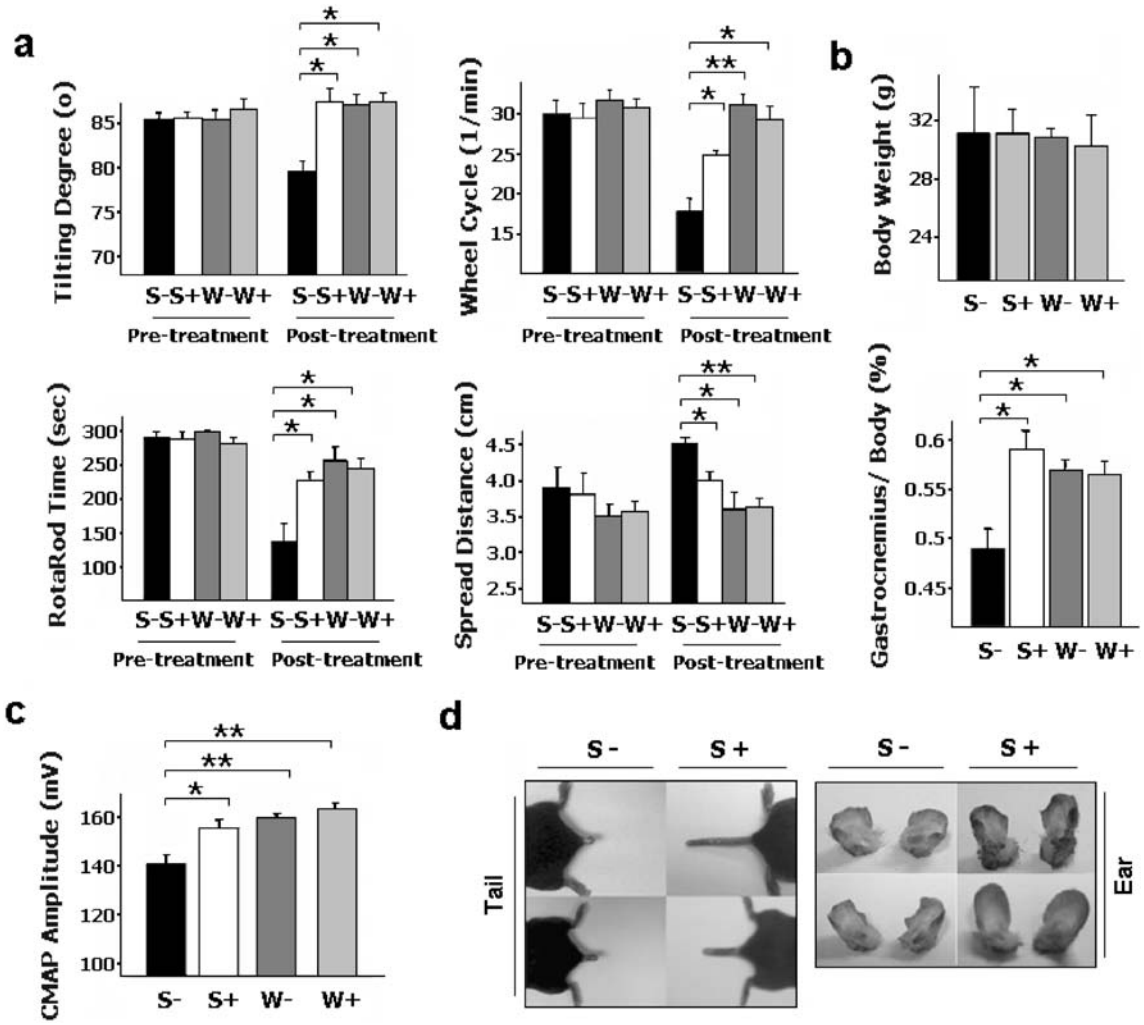

Fig. 1 Motor function, morphology, and electrophysiology of untreated SMA ($S-$, n=4), valproic acid (VPA)-treated SMA ($S+$, n=4), untreated wild-type ($W-$, n=5), and VPA-treated wild-type mice ($W+$, n=4). **a** VPA-treated SMA mice showed better motor performance than untreated SMA mice at 12 months in tilting, wheel running, RotaRod maintenance, and foot spreading tests. **b** Despite similar body weight between groups, VPA-treated SMA mice had a higher gastrocnemius/whole body weight ratio than untreated SMA mice. **c** Electric stimulation of the sciatic nerve generated a biphasic compound muscle action potential (*CMAP*) in gastrocnemius muscle. VPA-treated SMA mice showed a higher peak-to-peak CMAP amplitude than untreated SMA mice. **d** SMA mice with VPA treatment also had longer tails and milder degrees of ear border irregularity than untreated SMA mice. *P< 0.05; **P≤0.01

By 12 months of age, untreated SMA mice showed a significant reduction in CMAP amplitude in the gastrocnemius following stimulation of the sciatic nerve, compared to VPA-treated SMA mice and wild-type mice (Fig. 1c; P=0.02). In addition, morphological changes seen in SMA mice such as irregular ear borders and short tails were partially prevented by VPA treatment (Fig. 1d) [5].

Spinal motor neuron pathology

To confirm that VPA therapeutically targets motor neurons in SMA, 12-month-old SMA mice with or without 6 months of prior VPA treatment were sacrificed, and the lumbar spinal cord was removed. Staining with the motor neuron marker ChAT showed significantly higher motor neuron numbers in the lumbar spinal cord of VPA-treated SMA mice in comparison with untreated SMA mice (25±2.1 compared to 16±1.6 per section; P=0.02; Fig. 2a,d). However, as the number of large neurons was lower than normal in both treated and untreated SMA groups, H&E stain was used to further examine any differences in neuronal size distribution. The ratios of neuron density in VPA-treated SMA mice to untreated SMA mice in three size categories (400–600, 600–900, and >900 μm^2) were 1.5, 1.4, and 1.1, respectively (Fig. 2e), suggesting that VPA treatment was more likely to promote the survival of smaller neurons.

Retrograde neuronal tracing experiments, using intra-gastrocnemius injection of a fluorogold neurotracing agent showed that the surviving motor neurons did innervate muscle cells. The numbers of fluorescent motor neuron cell bodies in the anterior horn of lumbar spinal cord sections were significantly higher in VPA-treated SMA mice than in untreated SMA mice (12.5±0.5 vs. 7.9±1.3 per section; P=0.03; Fig. 2c,f). The number of motor neurons in VPA-treated SMA mice was about 90% of those in wild-type mice (P=0.2; Fig. 2d). However, the number of motor neuron cell bodies with an axon innervating hind limb muscles in VPA-treated SMA mice was only about 75% of those in wild-type mice (P=0.02; Fig. 2f). This indicates that while VPA could indeed rescue spinal motor neurons, some of these neurons (about 15%) seem to be functionless.

Muscle fiber and neuromuscular junction

We further examined changes in muscle fibers and neuromuscular junctions after VPA treatment. SMA and wild-type mice were treated with VPA from 6 to 12 months and 10 to 12 months of age, respectively. Myofibrillar ATPase staining of the quadriceps muscle showed obvious grouping of fiber types in SMA mice that was not present in wild-type mice, but VPA treatment attenuated the degree of this muscle denervation change (Fig. 3a–c). In addition, VPA treatment of SMA mice partially corrected the muscle abnormality with larger muscle fiber area (1,290±24 μm^2 compared to 1,117±22 μm^2; P= 0.02; Fig. 3g) and lower percentage of type I muscle fibers (56±3% compared to 75±5%; P=0.03; Fig. 3h) in comparison with untreated SMA mice.

Staining with the axonal marker neurofilament H and neuromuscular junction marker α-bungarotoxin showed a significantly higher percentage of innervated neuromuscular junction in the hamstring muscles of VPA-treated SMA mice in comparison with untreated SMA mice (79±5% compared to 62±3%; P=0.04; Fig. 3d,e,i). However, the percentage of innervated neuromuscular junctions in VPA-treated SMA mice was still lower than in wild-type mice (P= 0.04; Fig. 3e,f,i). Accumulated neurofilament often fills the neuromuscular junction in SMA [22]. After VPA treatment in SMA mice, this neurofilament accumulation was still frequently detected in neuromuscular junctions (Fig. 3e).

SMN protein analysis and *SMN2* gene expression

SMN protein levels in the spinal cord of SMA and wild-type mice after 6 and 2 months of VPA treatment, respectively, were analyzed. Western blots of SMN protein and α-tubulin showed a significant increase in SMN-immunoreactive protein after VPA treatment in SMA mice (0.35±0.03 vs. 0.26±0.02; P=0.04; Fig. 4a,b). However, SMN levels in both VPA-treated and untreated SMA mice were significantly lower than those in wild-type mice (P= 0.01; Fig. 4b). VPA treatment did not increase SMN protein levels in wild-type mice, which may be because pre-existing high SMN protein expression masked the small change due to VPA treatment. Up-regulation of SMN may be attributed to elevated levels of Htra2-β1 by VPA treatment in vitro [3]. However, Western blots of Htra2-β1 protein and α-tubulin showed similar Htra2-β1 levels in the spinal cord of SMA and wild-type mice with or without VPA treatment (Fig. 4a,b). To investigate the distribution of SMN, the spinal cord was stained for SMN antigens and the motor neuron marker ChAT (Electronic supplementary material, Fig. 1). A higher percentage of ChAT-immunopositive cells was also SMN immunopositive in the spinal cord of VPA-treated than untreated SMA mice (49±2% vs. 31±5%; P=0.03; Electronic supplementary material, Fig. 1j). SMN is usually concentrated within discrete nuclear compartments called gem bodies, where it plays an essential role in the assembly of the spliceosomal small ribonucleoproteins [23]. Gem numbers were also higher in VPA-treated mice than untreated SMA mice (1.1±0.2 vs. 0.5±0.1 per cell; P=0.04; Electronic supplementary material, Fig. 1k), implying that the additional SMN protein from VPA treatment may be functional. To exclude the possibility that the higher SMN levels in VPA-treated SMA

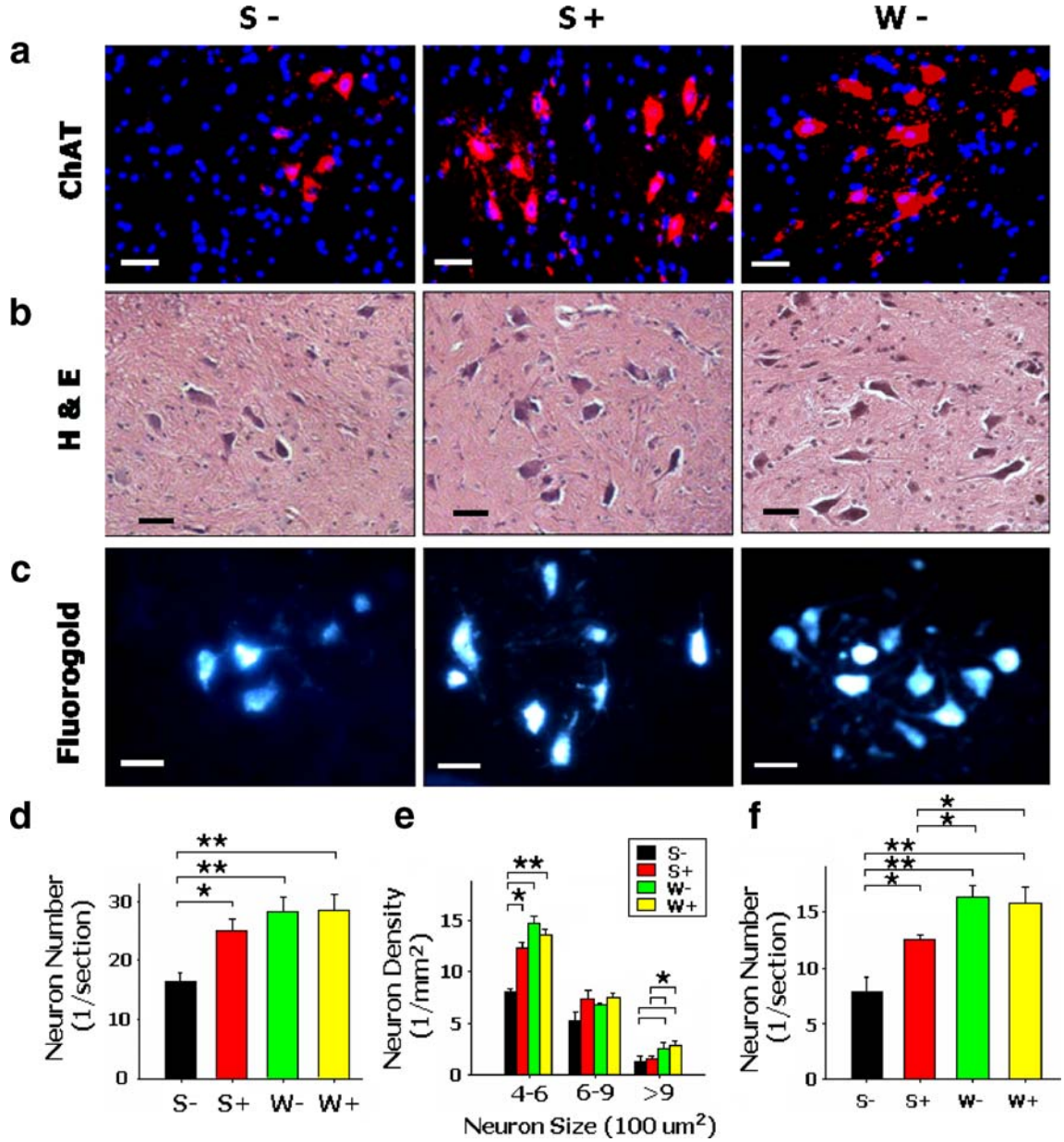

Fig. 2 Histological analysis of the spinal anterior horn in untreated SMA (*S*−, *n*=4), VPA-treated SMA (*S*+, *n*=4), untreated wild-type (*W*−, *n*=5), and VPA-treated wild-type mice (*W*+, *n*=4). **a**, **d** Spinal cord cross-sections were stained for nuclei with DAPI (*blue*) and for choline acetyltransferase (ChAT, *red*). VPA treatment significantly increased motor neuron number in spinal anterior horn of SMA mice. **b**, **e** Analyzing the neuronal density according to size (divided into three subgroups with areas of 400–600, 600–900, and >900 μm^2) revealed that small neurons were more likely to be rescued than large neurons after VPA treatment in SMA mice. H&E stain; **c**, **f** Fluorescence-labeled motor neurons with an axon innervating the gastrocnemius muscle in the spinal anterior horn by retrograde tracing following injection of fluorogold neurotracer into mouse gastrocnemius muscles. VPA treatment significantly increased fluorescence-positive cells in the anterior horn of SMA mice. Scale bars 50 μm; **P*<0.05; ***P*≤0.01

mice resulted only from higher motor neuron numbers in the spinal cord, we also treated SMA mice from 1 to 3 months of age (a period before the onset of motor neuron degeneration) with VPA. Western blots of SMN protein still showed a significant increase in SMN-immunoreactive protein following VPA treatment in SMA mice (0.42± 0.03 vs. 0.31±0.02; *P*=0.04).

Analyzing the *SMN* transcript levels by real-time PCR revealed a higher level of *SMN* expression (full-length and total transcripts) after VPA treatment (*P*=0.02; Fig. 4c) indicating significant promoter led activation of the *SMN2* transgene following VPA treatment. In addition, VPA treatment marginally increased the ratio of full-length to truncated *SMN* transcript (*P*=0.08; Fig. 4d) suggesting that

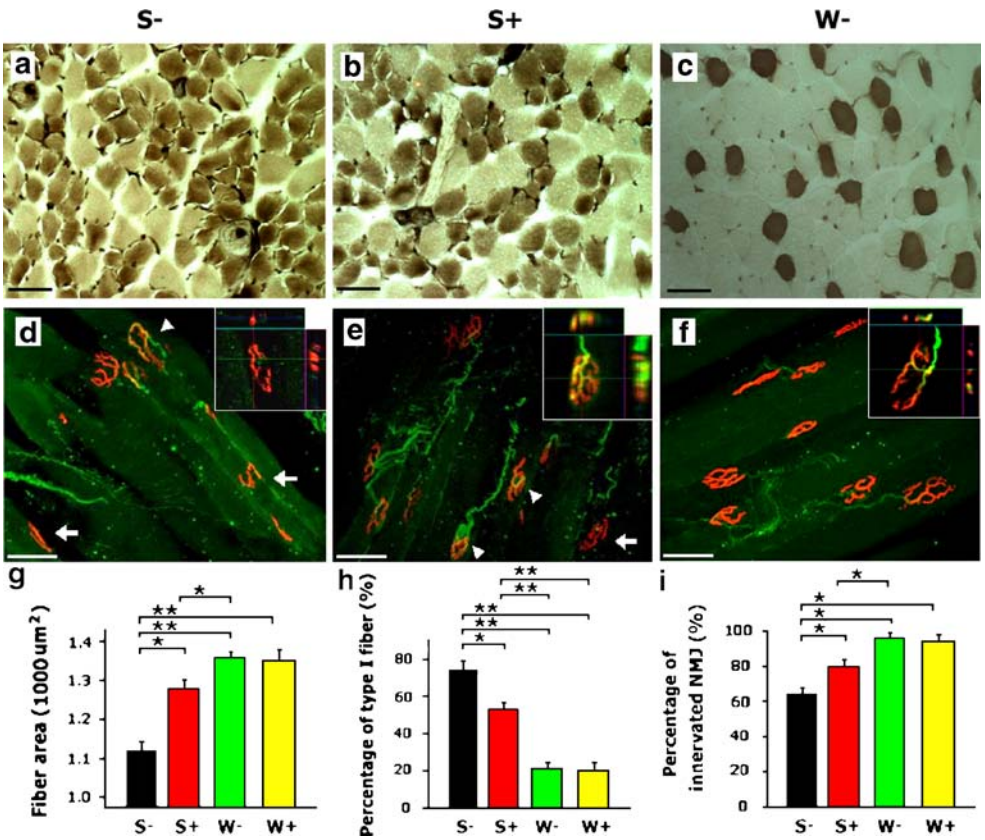

Fig. 3 Histological analysis of muscle fibers and neuromuscular junctions (*NMJ*) in untreated SMA (*S*−, *n*=3), VPA-treated SMA (*S*+, *n*=3), untreated wild-type (*W*−, *n*=3), and VPA-treated wild-type mice (*W*+, *n*=3). **a**–**c** ATPase stain at pH 4.3 differentiated type I (*dark*) and type II (*light*) fibers. VPA-treated SMA mice showed less muscle type grouping than untreated SMA mice. **d**–**f** Staining with axonal marker neurofilament H (*green*) and NMJ marker α-bungarotoxin (*red*) revealed some NMJ, especially in SMA mice, were non-innervated (*arrow*) or abundantly filled with neurofilament (*arrowhead*). **g** VPA-treated SMA mice showed larger muscle fiber area than untreated SMA mice. **h** VPA-treated SMA mice had a lower percentage of type I fiber than untreated SMA mice. **i** VPA-treated SMA mice showed higher percentage of innervated NMJ than untreated SMA mice. Scale bars 50 μm; **P*<0.05; ***P*≤0.01

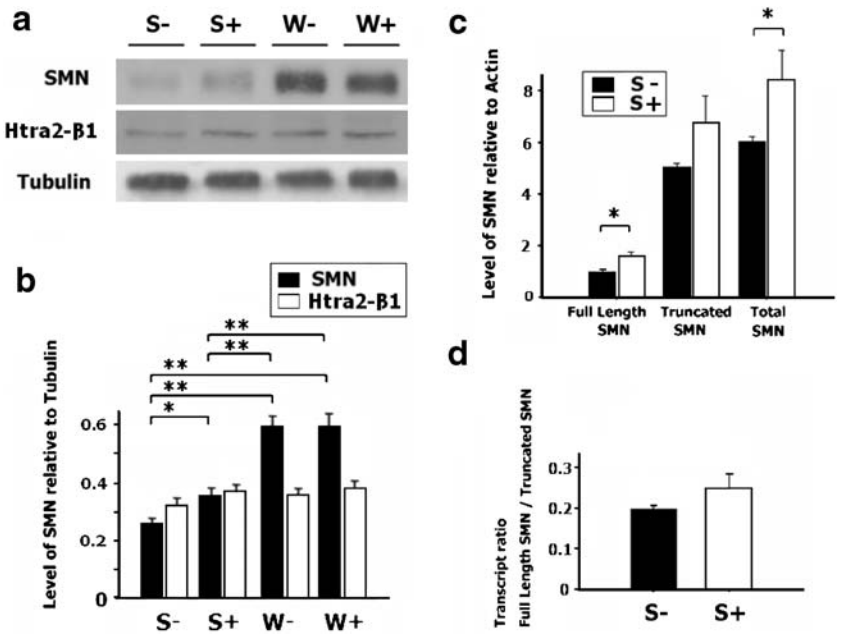

Fig. 4 Effect of VPA treatment on SMN protein and *SMN* mRNA levels in the spinal cords of untreated SMA (*S*−, *n*=4), VPA-treated SMA (*S*+, *n*=4), untreated wild-type (*W*−, *n*=5), and VPA-treated wild-type mice (*W*+, *n*=4). **a** Western blotting of SMN protein, Htra2-β1, and α-tubulin is shown. **b** Analyzing the ratio of SMN to α-tubulin levels (mean ± SEM) revealed a significant increase of SMN protein after VPA treatment. **c** Analysis of the *SMN* transcript levels (mean ± SEM) by real-time PCR revealed higher *SMN* expression (full-length and total transcripts) after VPA treatment. **d** VPA treatment marginally increased transcript ratio, for full-length and truncated *SMN*, which indicated VPA may convert truncated *SMN* to full-length *SMN*. **P*<0.05; ***P*≤0.01

VPA treatment probably restores correct *SMN2* pre-messenger RNA (mRNA) splicing.

As SMN has functional roles in muscles [24, 25], we also analyzed SMN expression in muscles by immunostaining gastrocnemius muscle sections. There was more SMN signal in muscles of VPA-treated than non-treated SMA mice (Electronic supplementary material, Fig. 2).

Anti-apoptotic factors

In 12-month-old untreated mice, levels of both Bcl-2 and Bcl-x_L in the spinal cord were lower in SMA mice than wild-type mice (P=0.04, Fig. 5). In 12-month-old SMA mice that had received 6 months of VPA treatment, levels of Bcl-2 (P=0.03) and phosphorylated ERK44/42 (P=0.04) in the lumbar spinal cord were 1.7 to 2 times higher than in untreated SMA mice. Unphosphorylated, native ERK44/42 levels were unaltered, suggesting that VPA may activate ERK and induce the expression of Bcl-2 in SMA spinal cord. In addition, we also found increased levels of Bcl-x_L in the spinal cord following VPA treatment (P=0.03). Since *Bcl-x_L* is a target gene of STAT5 [26], we also compared the levels of phosphorylated and non-phosphorylated STAT5, but found no difference in the two groups of SMA mice. Similar increases of Bcl-2, Bcl-x_L, and phosphorylated ERK44/42 levels (P=0.04) could also be found in the spinal cord of wild-type mice after 2 months of VPA treatment, indicating the VPA-related phenomenon was not exclusive to SMA.

To investigate the distribution of Bcl-2 and Bcl-x_L, spinal cord was immunostained for Bcl-2 or Bcl-x_L protein and the neuronal marker NeuN (Electronic supplementary material, Fig. 3). VPA-treated SMA mice had a higher percentage of NeuN/Bcl-2 double immunopositive cells (76±4% vs. 48±9%; P=0.04; Electronic supplementary material, Fig. 3g) or NeuN/Bcl-x_L double immunopositive cells (59±4% vs. 41±4%; P=0.04; Electronic supplementary material, Fig. 3h) in the spinal cord, compared with untreated SMA mice.

Neurogenesis and astrocyte proliferation

We further investigated the possibility of any neurogenic effects of VPA in SMA mouse spinal cords. BrdU was administered to 11-month-old SMA mice by intraperitoneal injection for three consecutive days, followed by VPA or no treatment for 4 weeks. Immunohistology of spinal cord showed a small number of BrdU/NeuN double positive cells in the VPA treatment group near the central canal (about two per 1,000 cells), but not the untreated group (Fig. 6a). There were no BrdU+/ChAT+ or BrdU+/vWF+ double labeled cells (data not shown). We did, incidentally, find a few GFAP+ cells mostly near the central canal which also stained for BrdU in both VPA-treated and untreated SMA mice (7±1.5 vs. 2±0.8 per 1,000 cells; P=0.03; Fig. 6b), indicating that VPA promotes astrocyte proliferation.

We finally examined the effects of VPA on myogenesis in SMA mice. After 6 months of VPA treatment, BrdU was injected intraperitoneally 6 h before sacrifice, then sections of gastrocnemius muscles were immunostained with antibodies raised against BrdU. Despite some obvious grouping of muscle fiber types, indicating axonal denervation, no BrdU+ cells were found (Fig. 6c).

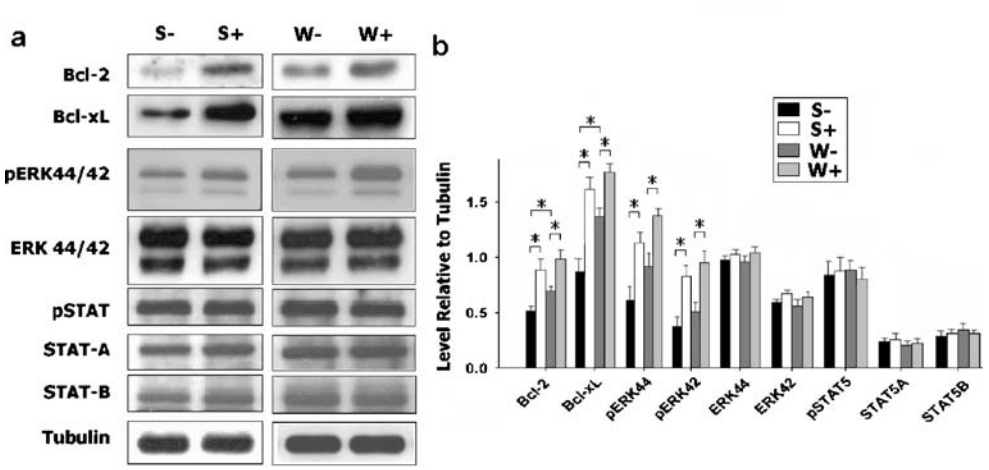

Fig. 5 Effects of VPA on anti-apoptotic factors in untreated SMA ($S-$, n=4), VPA-treated SMA ($S+$, n=4), untreated wild-type ($W-$, n=4), and VPA-treated wild-type mice ($W+$, n=4). **a** Western blot of spinal cord for Bcl-2, Bcl-x_L, phosphorylated and non-phosphorylated ERK44/42, and STAT5 and α-tubulin. **b** Analysis of the ratio of above proteins to α-tubulin levels (mean ± SEM) revealed lower Bcl-2 and Bcl-x_L protein expression in untreated SMA mice than untreated wild-type mice and a significant increase of Bcl-2, Bcl-x_L, and phosphorylated ERK44/42 protein levels after VPA treatment in SMA and wild-type mice. *P<0.05

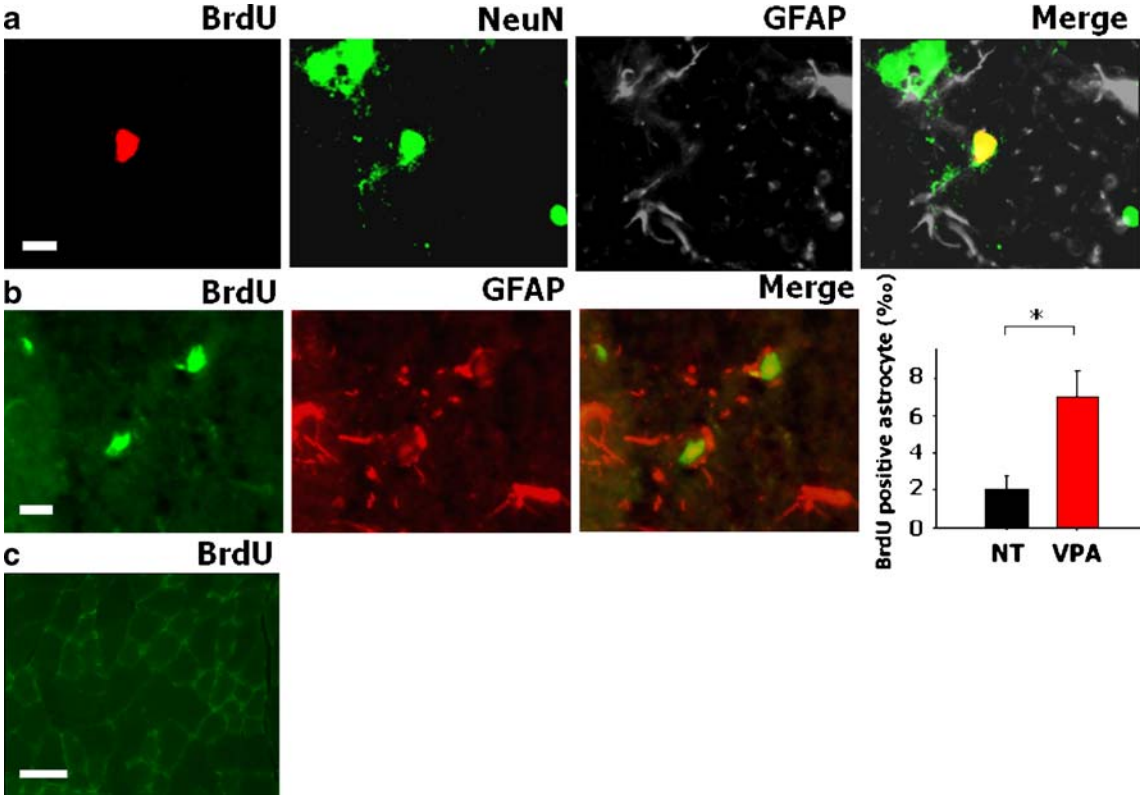

Fig. 6 Induction of neurogenesis and promotion of astrocyte proliferation by VPA treatment in SMA mice. **a** SMA mice were treated with BrdU followed by VPA or no treatment (NT) for 4 weeks. Sections of lumbar spinal cord were immunostained with antibodies raised against BrdU, NeuN, and GFAP. A few BrdU+ cells near the spinal canal of VPA-treated mice were also positive for NeuN. **b** There were more BrdU+/GFAP+ double labeled cells in VPA-treated mice than in untreated mice. Scale bars 10 μm. **P*=0.03. **c** After 6 months of VPA treatment, SMA mice were treated with BrdU 6 h before sacrifice. Sections of gastrocnemius muscles were then stained using antibodies raised against BrdU. No BrdU+ cells could be detected despite obvious grouping of muscle fiber types. Scale bars 100 μm

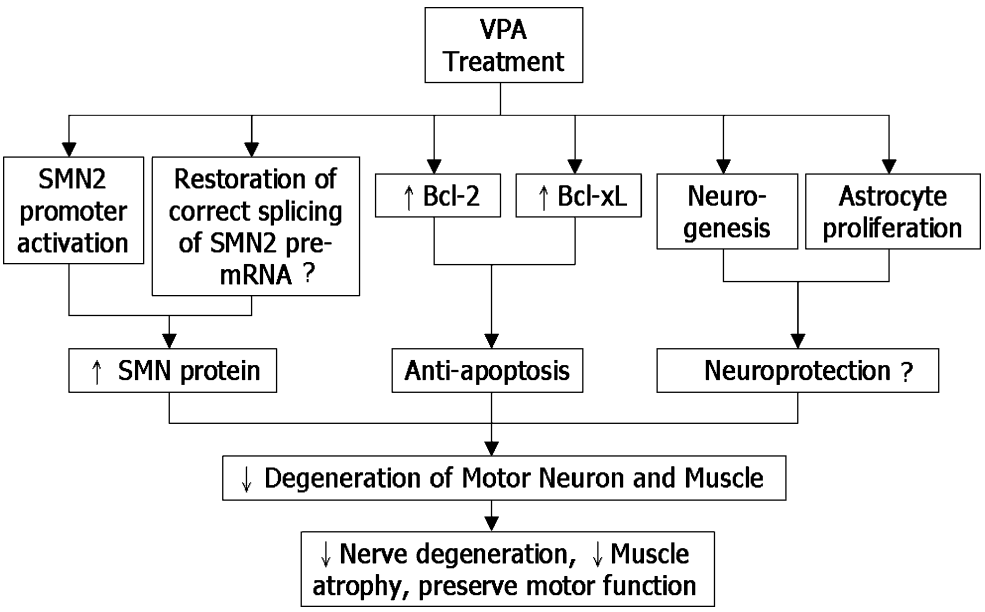

Fig. 7 Proposed rationale for therapeutic effects of valproic acid in spinal muscular atrophy

Discussion

We demonstrated that VPA has multiple therapeutic effects in SMA mice (Fig. 7). We confirmed that VPA elevated SMN protein levels in the spinal cord, through *SMN2* promoter activation and probable restoration of correct *SMN2* pre-mRNA splicing in vivo. The augmented SMN protein accumulated in the nucleus and appeared to be normally integrated into gem bodies. Because SMA is likely caused by insufficient levels of SMN protein in the motor neuron [27–30], the up-regulation of SMN seen here after VPA treatment seems to have meaningful therapeutic effects. Up-regulation of SMN may be attributed to elevated levels of Htra2-β1 by VPA treatment in vitro [3]. However, the levels of Htra2-β1 did not significantly increase in vivo, which may result from dilution of the effects by analysis of whole spinal cord extracts. As SMN also has functional roles in muscles [24, 25], the higher SMN expression in muscles of VPA-treated SMA mice may contribute to the positive therapeutic responses. VPA also increased the level of Bcl-2 and Bcl-x_L proteins in the spinal neurons, which may reduce motor neuron apoptosis in SMA. Furthermore, VPA probably induced neurogenesis and promoted astrocyte proliferation in the SMA mouse spinal cord, but the number of newly formed neurons was small and there were no newly formed motor neurons (absence of BrdU+/ChAT+ double labeled cells). The practical therapeutic contribution of VPA, if any, is more likely to be in terms of increased neuroprotection rather than frank neurogenesis.

By a combination of effects such as increased SMN protein levels, anti-apoptosis, and probable neuroprotection, the VPA-treated SMA mice showed considerably less degeneration of spinal motor neurons than untreated SMA mice. As such, their motor function was better preserved with less muscle denervation and atrophy than seen in untreated SMA mice. SMA mice have short tails and irregular ear border, possibly due to atrophy of tail muscles resulting in a failure in return of venous blood flow and chronic hypoxia [16]. These morphological changes were partially prevented by VPA treatment, which may be a result of VPA-related attenuation of neuron degeneration and muscle atrophy. Although the number of spinal neurons was similar in VPA-treated SMA mice and wild-type mice, some motor neurons in the VPA-treated SMA mice seemed to be functionless, without axons innervating muscles. In addition, muscle denervation changes and neurofilament accumulation in the neuromuscular junction could still be detected in VPA-treated SMA mice. Larger spinal motor neurons have previously been shown to be preferentially lost in SMA [5] and here we also showed that VPA preferentially rescued small motor neurons. Future development of treatment by VPA or other HDAC inhibitors must consider extending the therapeutic effectiveness, especially to larger motor neurons. VPA only increased SMA protein expression by one third in this study. However, trichostatin A could double SMN protein expression in SMA mice and is also an attractive drug for future clinical study [14].

VPA treatment increases the level of Bcl-2 in the frontal cortex of rats, perhaps through activation of ERK44/42 [11, 12]. We confirmed here that VPA induced both Bcl-2 up-regulation and phosphorylation-mediated ERK activation in the spinal cord of SMA and wild-type mice. In addition, VPA elevated Bcl-x_L without activation or induction of STAT5. To investigate the mechanism of Bcl-2 and Bcl-x_L up-regulation after VPA treatment, we treated SMA-like mouse embryonic fibroblasts with different concentrations of VPA. However, the levels of Bcl-2, Bcl-x_L, and phosphorylated ERK44/42 did not change after treatment (data not shown). The discrepancy between these in vivo and in vitro results may suggest that the up-regulation of anti-apoptotic factors by VPA is only achieved in neuronal cells and/or in an environment of spinal neuron–glial networks. On the other hand, the changes in Bcl-2 and Bcl-x_L could also be entirely secondary phenomena. Further studies using neuronal cell culture and Bcl-2 or Bcl-x_L transgenic SMA mice should try to elucidate the relationship between VPA treatment and these anti-apoptotic factors. We also demonstrated that Bcl-2 and Bcl-x_L were similarly down-regulated in the spinal cord of SMA mice as in SMA patients and these two anti-apoptotic factors would thus appear to be attractive therapeutic targets for the treatment of SMA [31, 32].

VPA has been shown to induce neurogenesis in the dentate gyrus of rat hippocampus through up-regulation of the ERK pathway [13]. Here we found that VPA can also induce neurogenesis in the spinal cord of SMA mice with activation of ERK44/42. The relationship between VPA-related neurogenesis and the ERK pathway in the spinal cord still needs to be investigated in further mechanistic studies. In the normal situation, endogenous progenitor cells reside close to the ependyma of the central canal of the spinal cord [33, 34]. Following spinal injury, these neural and glial progenitor cells have been shown to proliferate [35, 36]. In another motor neuron disease, amyotrophic lateral sclerosis (ALS), degeneration of motor neurons stimulates progenitor cell proliferation, migration, and differentiation in the spinal cord of ALS model mice [37–39]. However, we did not observe neurogenesis in the spinal cord of untreated type III-like SMA mice. This may be due to the fact that motor neuron degeneration in SMA is a less fulminant process than in ALS: while ALS patients normally die within 5 years of disease onset, this is not the case with type III SMA patients [40, 41].

We have previously demonstrated that SMA mice showed less degeneration of spinal motor neurons with relative preservation of motor function following VPA treatment from 1 month of age [5]. However, a clinical diagnosis of SMA is usually made following a patient's initial presentation of motor weakness, so here we investigated the efficacy of VPA commencement later in the disease progression. In this setting, VPA showed considerable therapeutic benefit in the mouse model, suggesting that VPA could be of benefit in SMA patients after the onset of motor neuron degeneration. The VPA serum levels in VPA-treated SMA mice were all less than 10 μg/ml, which is far less than the concentrations usually found in patients undergoing VPA treatment for epilepsy [42]. The results detailed here suggest that chronic low dose VPA may prove to be a viable, effective treatment for patients of SMA.

Acknowledgments This work was supported in part by the National Health Research Institute (grant NHRI-EX92-9029sp), National Taiwan University Hospital (grant NTUH-96M04), and Department of Medical Research of National Taiwan University Hospital. The authors thank Dr. Tzer-Bin Lin for electrophysiological equipment support.

Conflict of interest statement None.

References

1. Lefebvre S, Bürglen L, Reboullet S, Clermont O, Burlet P, Viollet L, Benichou B, Cruaud C, Millasseau P, Zeviani M et al (1995) Identification and characterization of a spinal muscular atrophy-determining gene. Cell 13:155–165
2. Wirth B (2000) An update of the mutation spectrum of the survival motor neuron gene (SMN1) in autosomal recessive spinal muscular atrophy (SMA). Hum Mutat 15:228–237
3. Brichta L, Hofmann Y, Hahnen E, Siebzehnrubl FA, Raschke H, Blumcke I, Eyupoglu IY, Wirth B (2003) Valproic acid increases the SMN2 protein level: a well-known drug as a potential therapy for spinal muscular atrophy. Hum Mol Genet 12:2481–2489
4. Sumner CJ, Huynh TN, Markowitz JA, Perhac JS, Hill B, Coovert DD, Schussler K, Chen X, Jarecki J, Burghes AH, Taylor JP, Fischbeck KH (2003) Valproic acid increases SMN levels in spinal muscular atrophy patient cells. Ann Neurol 54:647–654
5. Tsai LK, Tsai MS, Lin TB, Hwu, WL, Li H (2006) Establishing a standardized therapeutic testing protocol for spinal muscular atrophy. Neurobiol Dis 24:286–295
6. Brichta L, Holker I, Haug K, Klockgether T, Wirth B (2006) In vivo activation of SMN in spinal muscular atrophy carriers and patients treated with valproate. Ann Neurol 59:970–975
7. Tsai LK, Yang CC, Hwu WL, Li H (2007) Valproic acid treatment in six patients with spinal muscular atrophy. Eur J Neurol 14:e8–9
8. Weihl CC, Connolly AM, Pestronk A (2006) Valproate may improve strength and function in patients with type III/IV spinal muscular atrophy. Neurology 67:500–501
9. National Institutes of Health, US (2006) Valproic acid and carnitine in patients with spinal muscular atrophy. http://www.clinicaltrials.gov/ct/gui/show/NCT00227266. Accessed 29 Jan 2007
10. Bergeijk JV, Haastert K, Grothe C, Claus P (2006) Valproic acid promotes neurite outgrowth in PC12 cells independent from regulation of the survival of motoneuron protein. Chem Biol Drug Des 67:244–247
11. Chen G, Zeng WZ, Yuan PX, Huang LD, Jiang YM, Zhao ZH (1999) The mood-stabilizing agents lithium and valproate robustly increase the levels of the neuroprotective protein Bcl-2 in the CNS. J Neurochem 72:879–882
12. Einat H, Yuan P, Gould TD, Li J, Du J, Zhang L, Manji HK, Chen G (2003) The role of the extracellular signal-regulated kinase signaling pathway in mood modulation. J Neurosci 23:7311–7316
13. Hao Y, Creson T, Zhang L, Li P, Du F, Yuan P, Gould TD, Manji HK, Chen G (2004) Mood stabilizer valproate promotes ERK pathway-dependent cortical neuronal growth and neurogenesis. J Neurosci 24:6590–6599
14. Avila AM, Burnett BG, Taye AA, Gabanella F et al (2007) Trichostatin A increases SMN expression and survival in a mouse model of spinal muscular atrophy. J Clin Invest 117:659–671
15. Iezzi S, Padova MD, Serra C, Caretti G, Simone C, Maklan E, Minetti G, Zhao P, Hoffman EP, Puri PL, Sartorelli V (2004) Deacetylase inhibitors increase muscle cell size by promoting myoblast recruitment and fusion through induction of follistatin. Dev Cell 6:673–684
16. Hsieh-Li HM, Chang JG, Jong YJ, Wu MH, Wang NM, Tsai CH, Li H (2000) A mouse model for spinal muscular atrophy. Nat Genet 24:66–70
17. Tsai LK, Tai MS, Ting CH, Wang SH, Li H (2008) Restoring Bcl-x_L levels benefits a mouse model of spinal muscular atrophy. Neurobiol Dis. doi:10.1016/j.nbd.2008.05.014
18. Brooke MH, Kaiser KK (1970) Muscle fiber types: how many and what kind? Arch Neurol 23:369–379
19. Ting CH, Lin CW, Wen SL, Hsieh-Li HM, Li H (2007) Stat5 constitutive activation rescues defects in spinal muscular atrophy. Hum Mol Genet 16:499–514
20. Sumner CJ, Kolb SJ, Harmison GG, Jeffries NO, Schadt K, Finkel RS, Dreyfuss G, Fischbeck KH (2006) SMN mRNA and protein levels in peripheral blood, biomarkers for SMA clinical trials. Neurology 66:1067–1073
21. Shyu WC, Lin SZ, Yang HI, Tzeng YS, Pang CY, Yen PS, Li H (2004) Functional recovery of stroke rats induced by granulocyte colony-stimulating factor-stimulated stem cells. Circulation 110:1847–1854
22. Cifuentes-Diaz C, Nicole S, Velasco ME, Borra-Cebrian C, Panozzo C, Frugier T, Millet G, Roblot N, Joshi V, Melki J (2002) Neurofilament accumulation at the motor endplate and lack of axonal sprouting in a spinal muscular atrophy mouse model. Hum Mol Genet 11:1439–1447
23. Gubitz AK, Feng W, Dreyfuss G (2004) The SMN complex. Exp Cell Res 296:51–56
24. Rajendra TK, Gonsalvez GB, Walker MP, Shpargel KB, Salz HK, Matera AG (2007) A *Drosophila melanogaster* model of spinal muscular atrophy reveals a function for SMN in striated muscle. J Cell Biol 176:831–841
25. Cifuentes-Diaz C, Frugier T, Tiziano FD, Lacene E, Roblot N, Joshi V, Moreau MH, Melki J (2001) Deletion of murine SMN exon 7 directed to skeletal muscle leads to severe muscular dystrophy. J Cell Biol 152:1107–1114
26. Dumon S, Santos SC, Debierre-Grockiego F, Gouilleux-Gruart V, Cocault L, Boucheron C, Mollat P, Gisselbrecht S, Gouilleux F (1999) IL-3 dependent regulation of *Bcl*-xL gene expression by STAT5 in a bone marrow derived cell line. Oncogene 18:4191–4199
27. Parsons DW, McAndrew PE, Iannaccone ST, Mendell JR, Burghes AH, Prior TW (1998) Intragenic *telSMN* mutations: frequency, distribution, evidence of a founder effect, and modification of the spinal muscular atrophy phenotype by *cenSMN* copy number. Am J Hum Genet 63:1712–1723

28. Feldkotter M, Schwarzer V, Wirth R, Wienker TF, Wirth B (2002) Quantitative analyses of SMN1 and SMN2 based on real-time lightCycler PCR: fast and highly reliable carrier testing and prediction of severity of spinal muscular atrophy. Am J Hum Genet 70:358–368
29. Lefebvre S, Burlet P, Liu Q, Bertrandy S, Clermont, O, Munnich A, Dreyfuss G, Melki J (1997) Correlation between severity and SMN protein level in spinal muscular atrophy. Nat Genet 16: 265–269
30. Coovert DD, Le TT, McAndrew PE, Strasswimmer J, Crawford TO, Mendell JR, Coulson SE, Androphy EJ, Prior TW, Burghes AH (1997) The survival motor neuron protein in spinal muscular atrophy. Hum Mol Genet 6:1205–1214
31. Soler-Botija C, Ferrer I, Alvarez JL, Baiget M, Tizzano EF (2003) Downregulation of Bcl-2 proteins in type I spinal muscular atrophy motor neurons during fetal development. J Neuropathol Exp Neurol 62:420–426
32. Araki S, Hayashi M, Tamagawa K, Saito M, Kato S, Komori T, Sakakihara Y, Mizutani T, Oda M (2003) Neuropathological analysis in spinal muscular atrophy type II. Acta Neurophathol 106:441–448
33. Johansson CB, Momma S, Clarke DR, Risling M, Lendahl U, Frisen J (1999) Identification of a neural stem cell in the adult mammalian central nervous system. Cell 96:25–34
34. Martens DJ, Seaberg RM, van der Kooy D (2002) In vivo infusions of exogenous growth factors into the fourth ventricle of the adult mouse brain increase the proliferation of neuronal progenitors around the fourth ventricle and the central canal of the spinal cord. Eur J Neurosci 16:1045–1057
35. Mothe AJ, Tator CH (2005) Proliferation, migration, and differentiation of endogenous ependymal region stem/progenitor cells following minimal spinal cord injury in the adult rat. Neuroscience 131:177–187
36. Zai LJ, Wrathall JR (2005) Cell proliferation and replacement following contusive spinal cord injury. Glia 50:247–257
37. De Hemptinne I, Boucherie C, Pochet R, Bantubungi K, Schiffmann SN, Maloteaux JM, Hermans E (2006) Unilateral induction of progenitors in the spinal cord of hSOD1G93A transgenic rats correlates with an asymmetrical hind limb paralysis. Neurosci Lett 401:25–29
38. Ohta Y, Nagai M, Nagata T, Murakami T, Nagano I, Narai H, Kurata T, Shiote M, Shoji M, Abe K (2006) Intrathecal injection of epidermal growth factor and fibroblast growth factor 2 promotes proliferation of neural precursor cells in the spinal cords of mice with mutant human SOD1 gene. J Neurosci Res 84:980–992
39. Ke Y, Chi L, Xu R, Luo C, Gozal D, Liu R (2006) Early response of endogenous adult neural progenitor cells to acute spinal cord injury in mice. Stem cell 24:1011–1019
40. Talbot K, Davies KE (2001) Spinal muscular atrophy. Semin Neurol 21:189–196
41. Rowland LP, Shneider NA (2001) Amyotrophic lateral sclerosis. N Eng J Med 344:1688–1700
42. Brodie MJ, Dichter MA (1996) Antiepileptic drugs. New Engl J Med 334:168–175